Cancer Chemother Pharmacol (2011) 67:1145–1155
DOI 10.1007/s00280-010-1412-z

ORIGINAL ARTICLE

A combined pharmacokinetic model for the hypoxia-targeted prodrug PR-104A in humans, dogs, rats and mice predicts species differences in clearance and toxicity

Kashyap Patel · Steve S. F. Choy · Kevin O. Hicks · Teresa J. Melink · Nicholas H. G. Holford · William R. Wilson

Received: 6 April 2010 / Accepted: 16 July 2010 / Published online: 4 August 2010

Abstract
Background PR-104 is a phosphate ester that is systemically converted to the corresponding alcohol PR-104A. The latter is activated by nitroreduction in tumours to cytotoxic DNA cross-linking metabolites. Here, we report a population pharmacokinetic (PK) model for PR-104 and PR-104A in non-human species and in humans.
Methods A compartmental model was used to fit plasma PR-104 and PR-104A concentration–time data after intravenous (i.v.) dosing of humans, Beagle dogs, Sprague–Dawley rats and CD-1 nude mice. Intraperitoneal (i.p.) PR-104 and i.v. PR-104A dosing of mice was also investigated. Protein binding was measured in plasma from each species. Unbound drug clearances and volumes were scaled allometrically.
Results A two-compartment model described the disposition of PR-104 and PR-104A in all four species. PR-104 was cleared rapidly by first-order (mice, rats, dogs) or mixed-order (humans) metabolism to PR-104A in the central compartment. The estimated unbound human clearance of PR104A was 211 L/h/70 kg, with a steady state unbound volume of 105 L/70 kg. The size equivalent unbound PR-104A clearance was 2.5 times faster in dogs, 0.78 times slower in rats and 0.63 times slower in mice, which may reflect reported species differences in PR-104A *O*-glucuronidation.
Conclusions The PK model demonstrates faster size equivalent clearance of PR-104A in dogs and humans than rodents. Dose-limiting myelotoxicity restricts the exposure of PR-104A in humans to approximately 25% of that achievable in mice.

Keywords Hypoxia-activated prodrugs · Nitrogen mustards · Pharmacokinetics · PR-104 · Allometry

Introduction

Severe hypoxia is a prominent feature in solid tumours and drives many interrelated aspects of cancer biology. These include angiogenesis [1, 2], vasculogenesis [3], metastasis [4, 5], genomic instability [6], the switch to aerobic glycolysis [7], upregulation of pro-survival pathways under hypoxic stress [8], and selection of cells with genetic defects in death pathways [9]. In addition, hypoxic tumour cells are resistant to radiotherapy and chemotherapy [10, 11] and are therefore an important therapeutic target. There is ongoing interest, in this context, in the development of bioreductive prodrugs that are selectively activated by metabolic reduction when oxygen is absent [10, 12–16].

PR-104 is the first of the dinitrobenzamide mustard (DNBM) class of bioreductive compounds to enter clinical trial [17]. This phosphate ester was designed as a

Electronic supplementary material The online version of this article (doi:10.1007/s00280-010-1412-z) contains supplementary material, which is available to authorized users.

K. Patel · K. O. Hicks · W. R. Wilson (✉)
Faculty of Medical and Health Sciences, Auckland Cancer Society Research Centre, The University of Auckland, Private Bag 92019, Auckland, New Zealand
e-mail: wr.wilson@auckland.ac.nz

S. S. F. Choy · N. H. G. Holford
Department of Pharmacology and Clinical Pharmacology, Faculty of Medical and Health Sciences, The University of Auckland, Private Bag 92019, Auckland, New Zealand

T. J. Melink
Proacta Inc. 9255 Towne Centre Drive, Suite 520, San Diego, CA 92121-1870, USA

water-soluble "pre-prodrug", for systemic conversion to its corresponding alcohol, PR-104A (see Fig. 2 for structures). The latter is a bioreductive prodrug with 6- to 100-fold greater potency against human tumour cells under anoxic than aerobic (20% O_2) conditions [18, 19]. This selectivity is due to cytotoxic hydroxylamine and amine metabolites, formed following one-electron reduction by NADPH/cytochrome P450 oxidoreductase and other reductases, in an oxygen-sensitive manner [20]. PR-104A is also activated (at lower rates) to the same DNA cross-linking metabolites by aldo–keto reductase (AKR) 1C3 in aerobic tumour cells [19, 21]. Several features of PR-104A contribute to its notable activity against hypoxic (and aerobic) cells in human tumour xenografts [18, 19, 22]. One is that it penetrates efficiently into hypoxic tissue, as demonstrated in studies with multicellular layer cultures [22]. A second is that its hypoxia-dependent (one-electron) reduction is restricted to very low oxygen concentrations (K_m for $O_2 \sim 0.1$ μM) [22], not found in physiologically hypoxic normal tissues. Thirdly, high AKR1C3 expression can contribute to intra-tumour activation of PR-104A [21]. Furthermore, the active metabolites from PR-104A appear stable enough for local diffusion to adjacent oxygenated cells [18, 22–24].

Initial reports on the plasma pharmacokinetics (PK) of PR-104 indicate extensive conversion to PR-104A in rodents [18, 25] and in a phase I study in patients with advanced solid tumours [17, 26]. Recently, we have shown that the probability of tumour cell killing (log-surviving fraction by clonogenic assay) is proportional to the area under the concentration–time curve (AUC) for PR-104A in SiHa cultures.[1] The latter suggests PR-104A AUC as the relevant exposure variable for PR-104 cytotoxicity. In both rodents and humans, the plasma AUC of PR-104A is high enough to expect significant hypoxic tumour cell killing in vitro [18, 19, 22]. However, such comparisons are complicated by protein-binding differences in vitro and in vivo, as well as differences in concentration–time course between plasma and target (hypoxic or AKR1C3-expressing) tumour cells [22].

The main objective of the present study is to evaluate the plasma PK of unbound PR-104 and PR-104A in non-human species and humans, in part as a basis for comparing PR-104 anti-tumour activity across species. For this purpose, we develop a compartmental PK model that explicitly incorporates the hydrolysis of PR-104 to PR-104A. The model describes plasma concentration–time data from previously unreported mouse, rat and dog toxicokinetic studies, from a mouse study comparing intraperitoneal (i.p.) and intravenous (i.v.) dosing [18], from a recent phase I study [17] and unpublished data from a second phase I study [27]. A specific goal was to compare species differences in PR-104 and PR-104A clearances using allometric (3/4 power) scaling for body size [28]. Finally, to help inform design of ongoing non-human studies, we use the model to estimate PR-104 doses in mice, rats and dogs that provide PR-104A exposure equivalent to that achievable in humans.

[1] Patel K, Foehrenbacher A, Secomb TW, Wilson WR, Hicks KO. A spatially resolved pharmacokinetic/pharmacodynamic model for hypoxic activation and bystander killing by the bioreductive prodrug PR-104. Manuscript *in preparation*.

Materials and methods

Drugs and reagents

PR-104 (MW 579 as the free acid; FA) and PR-104A (MW 499) were synthesised as previously reported [29]. For non-human studies, the batches of PR-104 used (FA11 for mice and FA MPD-A-125(1) for rats and dogs) had purity >96%, based on HPLC with absorbance detection at 254 nm. Purity of the clinical API (Proacta Inc.) was 95%. The PR-104A (batch NC9) used in mouse studies was >97% pure. All other solvents were commercially available and of analytical grade.

Animals

Mouse experiments were conducted at the University of Auckland (New Zealand) under ethics approval AEC R279. Rat and dog studies were performed at LAB Preclinical Research Inc. (Quebec, Canada) and complied with the GLP regulations of the Food and Drug Administration (FDA, USA). Specific pathogen-free CD-1 Foxn1^{nu} athymic mice (Charles River Laboratories, Wilmington, MA) were bred at the University of Auckland and housed (≤6/cage) in Techniplast microisolator caging. Sprague–Dawley rats (Charles River Inc., Canada) and Beagle dogs (Gaoyao Kangda Laboratory Animals Science and Technology Ltd., China) were individually housed in stainless steel cages. Room environments were controlled at a temperature of 21°C and humidity 30–70%, with a 12-h light/dark cycle. Standard certified commercial diet (Teklad 2018c for rats, 2018i for mice or 8727c for dogs) and water was provided ad libitum. Rodents were identified by ear tags and dogs by an ear tattoo. At the time of experiments, mice weighed 21–30 g (7–9 weeks of age), rats 184–364 g (8–9 weeks of age) and dogs 10.2–13.3 kg (7–8 months of age).

Drug formulation and dosing

For non-human studies, PR-104 free acid was dissolved in PBS + 1 equivalent $NaHCO_3$. PR-104A was dissolved in

DMSO and diluted in PBS (to 1% DMSO) for dosing mice. All dosing solutions were prepared fresh and filtered through 0.2-μm acrodisc filters. These were then held at room temperature in amber vials and used within 3 h from the time of preparation. In rodents, drug was administered by i.v. bolus injection via a lateral tail vein; the dose volumes were 0.005–0.01 mL/g (mice) and 0.00583 mL/g (rats). Mouse i.p. dosing volumes were 0.01–0.02 mL/g. Dogs were treated with i.v. infusion (Baxter Flo Gard pump) through an indwelling catheter (Abbocath®) inserted into a cephalic vein; the rate of infusion was 10 mL/min at a volume of 10 mL/kg. For human studies, PR-104 vials (400 mg) were reconstituted with 2 mL of sterile water, diluted in 250 mL of 5% dextrose and administered by i.v. infusion over 1 h.

Non-human toxicology

The maximum-tolerated dose in mice was determined as previously using 1.33-fold dose escalation steps [18]. Rats (15/sex/dose) and dogs (5/sex/dose) received PR-104 weekly for 4 consecutive weeks and were monitored (clinical signs, body weight, clinical chemistry and haematology) for 28 days after the last dose. The doses tested were 50, 225 and 350 mg/kg/dose (rats) and 15, 50 and 150 mg/kg/dose (dogs). Control groups (0 mg/kg/dose) were treated with PBS as the vehicle. Animals were then terminated for necropsy and histopathology of selected tissues.

Non-human pharmacokinetic studies

Female mice were administered PR-104 (32.6 and 326 mg/kg) or PR-104A (28.0 mg/kg) by i.v. or i.p. bolus injection. Rats (9/sex/dose) and dogs (3/sex/dose) from the same cohorts as in the above toxicology studies were sampled for PK on days 1 and 22. Blood was collected by cardiac puncture under terminal CO_2 anaesthesia in mice and serially from the jugular vein in rats and dogs. Only three rats were assayed at each time point to minimise any changes in blood volume. Samples were placed into chilled microcentrifuge tubes containing EDTA as the anticoagulant, and plasma immediately prepared by centrifugation (2,500–3,000$\times g$; 3 min). All samples were then stored at −80°C for subsequent LC/MS or LC/MS/MS analysis.

Human pharmacokinetic studies

The plasma PK of PR-104 was evaluated in two phase I studies in patients with advanced solid tumours. In one study (PR-104-1001), 27 patients received doses (using a once-every-3-week schedule) ranging from 135 to 1,400 mg/m^2; the study design, patient characteristics and toxicity are described elsewhere [17]. The PK analysis here includes 25 patients from a second study (PR-104-1003), in which PR-104 was administered at 140–1,100 mg/m^2 prior to gemcitabine or docetaxel treatment [27]. The plasma PK of PR-104 and PR-104A was investigated only on the first cycle for both studies.

Measurement of plasma PR-104 and PR-104A concentrations

The analytical methods for PR-104 and PR-104A in plasma have been previously reported [25]. Briefly, rat, dog and human plasma were precipitated using cold methanol/ammonium acetate/acetic acid (1000: 3.5: 0.2, v/w/v); only cold methanol was used to precipitate mouse samples. Tetradeuterated isotope (humans and mice) or diethyl analogue (rats and dogs) internal standards were added to plasma extracts prior to analysis. Rat, dog and human samples were analysed by a rapid and sensitive LC/MS/MS method; lower limits of quantitation (LLOQ) were 0.009 μM for PR-104 and 0.1 μM for PR-104A (0.01 μM in rat plasma). A high chromatographic resolution LC/MS assay was used for the analysis of mouse plasma (LLOQ of 0.3 μM for both compounds). Data below the LLOQ were included in the PK analysis, except for PR-104 concentrations beyond 1 h (rats) and 2 h (dogs and humans), because of suspicions of contamination from previous samples. All measured values were included in mouse data sets for both PR-104 and PR-104A.

Determination of plasma protein binding

Methanol stock solutions of PR-104 or PR-104A were added to heparinised plasma to achieve concentrations ranging from 1.73 to 1,730 μM (1–1,000 μg/ml). At each concentration, aliquots (1.0 mL) were loaded into three Centrifree ultrafiltration cartridges (Millipore, MA) and centrifuged (1,300$\times g$; 15 min). The filtrate and retentate were then extracted and analysed by LC/MS/MS. For each species, unbound fractions of each compound in plasma were averaged, and used to predict the measured total drug concentrations from the unbound concentration predictions.

Pharmacokinetic modelling

Non-compartmental PK parameters were estimated using WinNonlin (version 5.0); AUC values were calculated using the log trapezoidal rule with extrapolation of the terminal slope to infinity by linear regression using 3–4 data points. The extrapolated component comprised 4–7%

of the total AUC. Hypothesis testing was undertaken by *t* test using log-transformed AUC.

A compartmental model was used to describe plasma concentration–time data from all four species. Parameter values were standardised for a body weight (BW) of 70 kg using an allometric model (Eq. 1) to allow cross-species comparison of the estimates [28, 30].

$$P = P\text{std} \cdot \left(\frac{\text{BW}}{\text{BW}_{\text{std}}}\right)^{\text{PWR}} \quad (1)$$

where P is the parameter prediction for an animal with weight BW, Pstd is the parameter value in a 70-kg animal, and BW_{std} is the standard weight (70 kg) of an adult human.

Unbound drug volumes (V) were scaled allometrically with PWR = 1, and unbound clearances (CL) with PWR = 3/4. These PWR exponents were selected due to their strong theoretical and empirical basis for clearance and volume of distribution [31–33]. Both first-order and mixed-order processes were tested to describe PR-104A formation from PR-104 in the central compartment. For both compounds, the model was parameterised in terms of central and inter-compartmental clearances, as well as volumes of distribution for central and peripheral compartments. Based on biochemical grounds, all elimination of PR-104 was assumed to be due to conversion to PR104A. This assumption allows PR-104A disposition parameters to be identified. Administration of PR-104A to mice allowed direct estimation of PR-104A disposition without the conversion assumption.

The PK model after i.p. injection in mice assumed first-order conversion of PR-104 to PR-104A in the peritoneal cavity, followed by first-order absorption of both compounds. Equation 2 was used to calculate the unbound AUC of PR-104 and PR-104A in plasma from zero to infinite time.

$$\text{AUC}_{\text{u}} = \frac{\text{Dose}}{\text{CL}_{\text{u}}} \quad (2)$$

where AUC_{u} is the unbound AUC, CL_{u} the unbound clearance and Dose the PR-104 dose. Population parameter variability (PPV) was assumed to follow a lognormal distribution, with its magnitude expressed as an apparent coefficient of variation (CV). In the human model, PPV was described only by between-subject variability (BSV), because PK was only studied on one occasion. For rat and dog models, PPV was partitioned into between-occasion variability (BOV) and BSV, with BOV describing within-subject variability in animals treated on day 1 and day 22. To account for differences between nominal infusion durations and the duration that best described the data, the PPV for infusion duration (PPV_{D1}) was estimated in humans and dogs.

Residual unidentified variability (RUV) was modelled using a combined proportional (RUV_CV) and additive (RUV_SD) random error.

Population parameter estimates were obtained by non-linear mixed-effects modelling (NONMEM version 7; Intel Visual Fortran compiler version 10.1) using the first-order conditional estimation method with interaction and ADVAN13 to solve differential equations. A convergence criterion of three significant figures was used. The NONMEM objective function value (OBJ) and visual predictive checks (VPC) were used to evaluate goodness of fit.

The structural model for each animal species was determined by fitting the data for each species separately. Once the structure had been defined, all data (including both PR-104 and PR-104A dosing in mice) were combined using BW of each individual, and model parameters were estimated simultaneously from all species. Model evaluation was performed using untransformed and prediction-corrected VPC.[2] One thousand data sets were simulated from the final parameter estimates using the original data as a template to define an empirical covariate distribution. The median and 90th percentile of simulated concentrations were then computed and plotted against observed values.

Results

Determination of maximum-tolerated dose and dose-limiting toxicities

Dose-ranging studies in non-human species and in humans provided the estimates of maximum-tolerated doses (MTD) shown in Table 1. For mice and rats, the MTD was the highest dose that did not cause lethality or unacceptable clinical toxicity. All dogs survived the highest dose tested (150 mg/kg), without clinical signs except for a transient fall in food consumption and body weight in females. However, this dose was considered the MTD due to significant myelotoxicity (Fig. S1), which manifested as dose-dependent reversible effects on neutrophils, lymphocytes, erythrocytes, haemoglobin, reticulocytes and platelets (data not shown). Similar dose-related myelotoxicity was observed in rats (Fig. S2) and humans, for which dose-limiting toxicities were neutropenia, infection without neutropenia and fatigue [17]. Histopathology showed marked lymphoid hypoplasia in rats and mice, consistent with dose-limiting myelotoxicity, although gastrointestinal

[2] Bergstrand M, Hooker AC, Wallin JE, Karlsson MO. Prediction corrected visual predictive checks. http://www.go-acop.org/sites/all/assets/webform/PC_VPC_Abstract_ACoP_090715_final.doc.

Table 1 Maximum-tolerated doses (MTD) of PR-104 in humans, dogs, rats and mice, and AUC estimates using the log trapezoidal rule

Species	Route	Infusion	Dosing schedule	MTD (per dose)		Non-compartmental $AUC_{0-\infty}$ (μM h)[a]		
				mg/kg	mg/m^2	*N*[b]	PR-104	PR-104A
Humans	i.v.	60 min	Once every 3 weeks	28[c]	1,100[c]	6	5.2 ± 0.3	16.9 ± 2.4
Dogs	i.v.	10 min	Weekly for 4 weeks	150	2,678	6	9.9 ± 0.8	25.1 ± 0.9
Rats	i.v.	Bolus	Weekly for 4 weeks	225	1,328	6	35.2 ± 2.3	32.1 ± 1.1
Mice	i.v.	Bolus	Single dose	434	1,208	–	68[e]	83[e]
Mice	i.p.	Bolus	Single dose	770[d]	2,144	–	34[f]	120[f]
Mice	i.p.	Bolus	Every 4 days × 3	617[d]	1,718	–	–	–

[a] For first dose, combining data for both sexes. Values are mean and SEM for the unbound compounds

[b] Number of subjects

[c] MTD for single-agent PR-104, from study PR104-1001 [17]

[d] From [18]

[e] Determined at a PR-104 dose of 326 mg/kg i.v. (Table S4) and scaled linearly to 434 mg/kg

[f] Determined at a PR-104 dose of 326 mg/kg i.p. (Table S4) and scaled linearly to 770 mg/kg

Table 2 Plasma protein binding of PR-104 and PR-104A, evaluated in human, dog, rat and mouse plasma by ultracentrifugation

Species	PR-104		PR-104A	
	Concentration (μM)	% unbound drug	Concentration (μM)	% unbound drug
Human	1.73	29.4 ± 2.5	2	36.1 ± 0.6
	17.3	29.3 ± 2.8	20	40.3 ± 2.4
	173	26.7 ± 5.3	200	52.8 ± 1.8
Dog	17.3	29.6 ± 0.4	20	64.4 ± 0.6
	173	25.7 ± 4.3	200	66.4 ± 11.4
Rat	173	36.7 ± 3.6	20	60.1 ± 13.3
	1730	36.8 ± 1.5	200	61.4 ± 1.1
Mouse	173	38.4 ± 2.6	20	66.8 ± 1.7
	1730	63.0 ± 6.3	200	72.9 ± 2.4

Values are mean ± SEM for triplicate determinations

and hepatic pathology was also observed at doses above the MTD in both species (data not shown).

In vitro plasma protein binding

Plasma protein binding of PR-104 and PR-104A is summarised in Table 2. PR-104 was moderately bound to plasma proteins (mean 32% unbound), at the one concentration (173 μM) tested in all species. The unbound fraction was slightly higher in rodents than dogs or humans, and no clear concentration dependence was evident. For PR-104A, plasma protein binding was even lower across species (mean 58% unbound), with a slight concentration dependence in mouse and human plasma.

Plasma PK in non-human species and humans

Total drug concentration–time profiles in plasma were measured in humans, dogs, rats and mice after the first dose at a range of i.v. dose levels. Concentration–time values at the highest dose level (approximating the MTD) are illustrated in Fig. 1; non-compartmental parameters based on unbound concentrations are reported for all dose levels and for repeat doses in Tables S1–S5. The data confirm rapid conversion of PR-104 to PR-104A in all four species with no major non-linearity with dose (although a trend to decreasing PR-104 clearance with dose occurs in all three non-human species). In the most extensively studied non-human species (rats and dogs), no differences were discerned between sexes or between the first and 4th dose in a weekly dosing schedule (Tables S2 and S3). For PR-104A, terminal half lives (averaged over all subjects) increased in the order: dogs (0.21 h) < mice (0.24 h) < rats (0.45 h) < human (0.75 h), suggesting a PK difference in dogs that does not track with expected allometric (body size) relationships. Non-compartmental unbound AUC values for PR-104A at the monotherapy MTD in humans determined in the PR-104-1001 study (Table 1) were ~5-fold lower than for mice, and intermediate for the other non-human species.

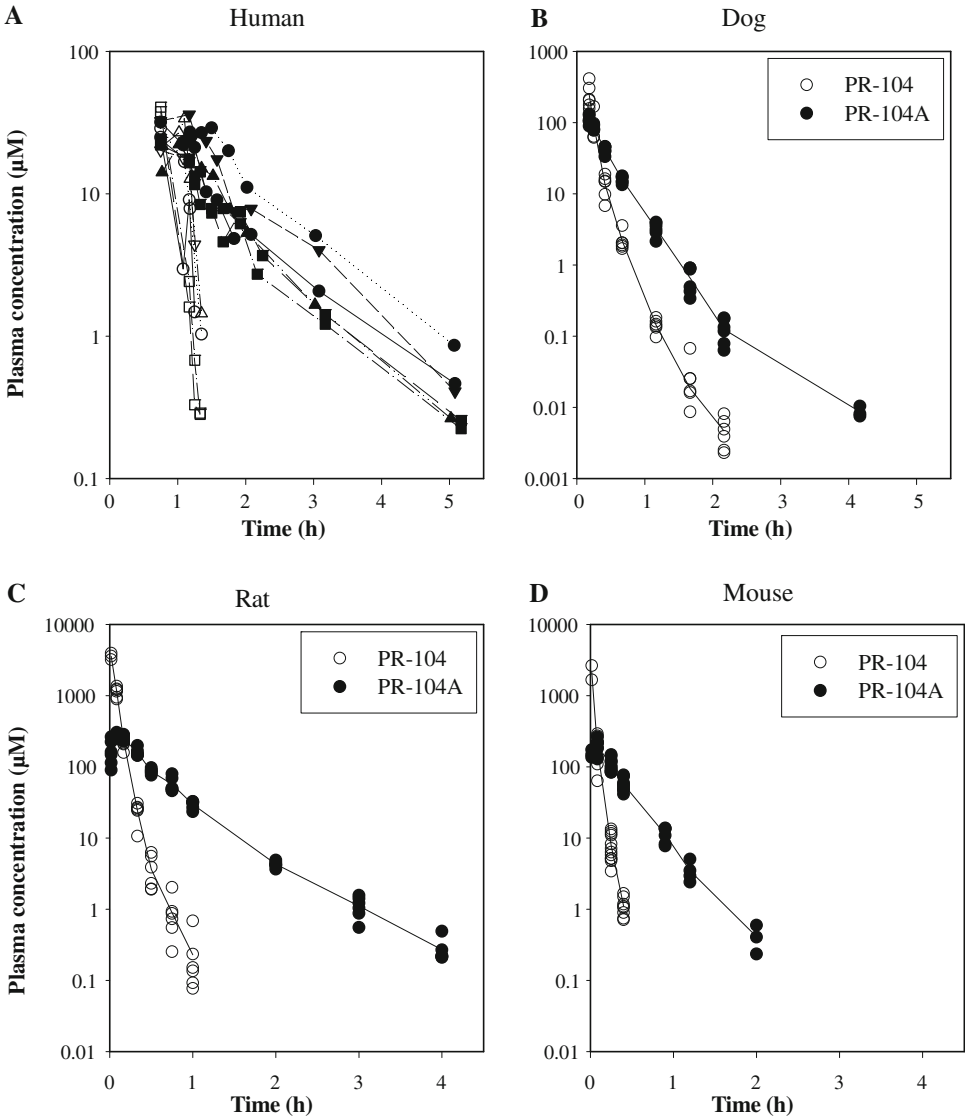

Fig. 1 Plasma concentration–time data of PR-104 (open symbols) and PR-104A (filled symbols), following i.v. PR-104 administration at the single-agent maximum-tolerated doses (MTD) of (**a**) 1,100 mg/m^2 in humans, (**b**) 150 mg/kg in dogs, (**c**) at 225 mg/kg in rats, and (**d**) 326 mg/kg (75% of the single-dose i.v. MTD) in mice. Dosing was by 60-min infusion in humans, 10-min infusion in dogs, and injection of bolus in rodents. Lines join points for the same individual (humans), or group means for non-human species

The PK of PR-104A in mice was also assessed following its dosing in 1% DMSO/PBS at 28 mg/kg (Fig. S3 and Table S5). This demonstrated a similar half-life to that when PR-104A was formed from the same molar dose of PR-104 (32.6 mg/kg), but the geometric mean AUC for PR-104A was 42% lower when formed from PR-104; this difference was statistically significant ($P = 0.004$).

Cross-species compartmental model

The structural model shown in Fig. 2 was fitted to the PR-104 and PR-104A concentration–time data simultaneously. This two-compartment model provided a better fit than one-compartment models for both PR-104 and PR-104A. The conversion of PR-104 to PR-104A was describable by a first-order process in non-human species. In humans, the fit was better described by a mixed-order process with a decrease in OBJ of 65 units compared with a first-order process. There was no support for an additional parallel first-order process in humans. Elimination of PR-104A appeared to be first-order in all species with no evidence for mixed order elimination. The OBJ value decreased 15 units when 28.6% of the clearance of PR-104 in mice was assumed to occur by a second first-order pathway. Because this second pathway is not identifiable as a model parameter for other species, the parameter estimates presented in Table 3 were derived by fitting the combined data for all species simultaneously and assumed 100% conversion of PR-104 to PR-104A. There was no evidence for a sex difference in the elimination of either PR-104 or PR-104A. Model parameters describing between- and within-subject variability and residual error are provided in Table 4. Between-subject variability in inter-compartmental clearance and peripheral volume of distribution was not estimable.

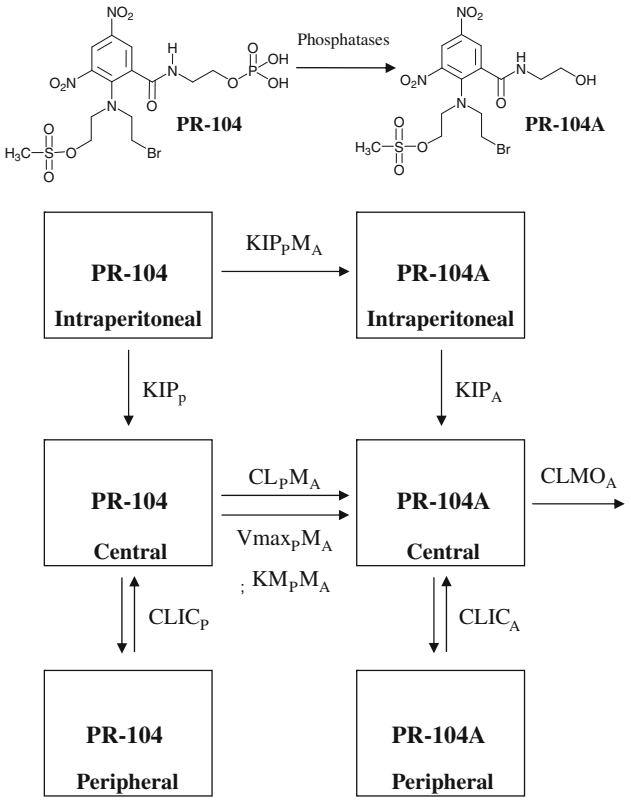

Fig. 2 Structural formulae of PR-104 and PR-104A (*top*), and schematic representation of the compartmental model (*bottom*) used to describe the plasma PK of both compounds across four species (human, dog, rat and mouse). The model parameters are defined in Table 3

Model evaluation

The VPCs for each species are shown in Fig. 3 (PR-104) and Fig. 4 (PR-104A). The model prediction percentiles (5th, median, 95th) closely match the corresponding observation percentiles. This confirms the suitability of the model to describe both PR-104 and PR-104A disposition in all species.

Discussion

PR-104 was designed to provide intra-tumour formation of cytotoxic nitrogen mustard metabolites and embodies two different prodrug concepts. The phosphate "pre-prodrug" PR-104 represents a formulation strategy for systemic delivery of the less-soluble PR-104A, which is a prodrug that is activated by nitroreduction within the target (tumour) tissue [18–21]. The present study demonstrates rapid and extensive conversion of PR-104 to PR-104A across species and provides a common structural model that adequately describes plasma concentration–time profiles of both compounds.

Interest in developing a compartmental model with allometrically scaled parameters was stimulated in part by the observation that the terminal half-life of PR-104A (dogs < mice < rats < human) did not show body size relationships expected from allometric theory if there were no species difference in size equivalent parameters (mice < rats < dogs < humans). There is a strong theoretical and empirical basis for scaling volumes linearly with BW and clearances to $BW^{0.75}$ [31]; the latter is consistent with strong evidence for power law scaling of metabolic rates in mammals over the size range of interest [32–34].

The final PK model assumed total conversion of PR-104 to PR-104A in the central compartment, with no other elimination pathway for PR-104. We note, however, that

Table 3 Unbound PR-104 and PR-104A pharmacokinetic parameter estimates based on the model of Fig. 2 by simultaneous fitting of combined data from all species

Compound	Parameter	Description	Units	Human	Dog	Rat	Mouse
PR-104	VC_P	Central volume of distribution for PR-104	L/70 kg	33.2	37.2	31.2	46.1
	CL_PM_A	First-order formation of PR-104A	L/h/70 kg	–	1,138	182	205
	$Vmax_PM_A$	Saturable $V_{max.}$ of PR-104 to PR-104A	mmol/h/70 kg	13.5	–	–	–
	KM_PM_A	Saturable K_m of PR-104 to PR-104A	μM	23.6	–	–	–
	$CLIC_P$	Inter-compartmental PR-104 clearance	L/h/70 kg	11.9	125	5.24	20.0
	VP_P	Peripheral volume of distribution for PR-104	L/70 kg	51.4	32.2	2.84	9.10
	KIP_P	First-order i.p. absorption of PR-104	1/h	–	–	–	2.15
	KIP_PM_A	First-order i.p. conversion of PR-104 to PR-104A	1/h	–	–	–	2.04
PR-104A	VC_A	Central distribution volume for PR-104A	L/70 kg	50.4	50.0	178	153
	$CLMO_A$	First-order clearance of PR-104A	L/h/70 kg	211	525	164	133
	$CLIC_A$	Inter-compartmental first-order clearance	L/h/70 kg	101	523	37.1	94.8
	VP_A	Peripheral volume of distribution for PR-104A	L/70 kg	54.1	102	65.5	82.2
	KIP_A	First-order i.p. absorption of PR-104A	1/h	–	–	–	3.34

P and A subscripts refer to parent (PR-104) and metabolite (PR-104A), respectively

Table 4 Variability in PR-104 and PR-104A pharmacokinetic parameter estimates and residual error, obtained by simultaneous fitting of combined data from all species

Parameter	Description	Variability in PK Parameter estimates[a]			
		Human	Dog	Rat	Mouse
PPV_{D1}	Between-subject variability in infusion duration	0.0689	0.0339	–	–
$BSVVC_P$	Between-subject variability in VC_P[b]	0.511	0.567	–	–
$BSVCL_PM_A$	Between-subject variability in CL_PM_A	–	0.307	0.275	–
$BSVVmax_PM_A$	Between-subject variability in $Vmax_PM_A$	0.113	–	–	–
$BSVKM_PM_A$	Between-subject variability in KM_PM_A	0.373	–	–	–
$BSVVC_A$	Between-subject variability in VC_A[c]	0.590	0.0386	–	–
$BSVCLMO_A$	Between-subject variability in $CLMO_A$	0.279	0.190	0.155	–
$BOVVC_P$	Between-occasion variability in PR-104 VC_P	–	0.109	–	–
$BOVCL_PM_A$	Between-occasion variability in PR-104 CL_PM_A	–	0.133	–	–
$RUVCV_P$	CV of PR-104 residual error	0.401	0.375	0.437	0.433
$RUVCV_M$	CV of PR-104A residual error	0.212	0.0617	0.259	0.303
$RUVSD_P$	SD of PR-104 residual error (μM)	0.0110	0.0076	0.0122	0.0194
$RUVSD_M$	SD of PR-104A residual error (μM)	0.0704	0.0088	0.0287	0.245

[a] Variability is shown as the square root of the OMEGA and SIGMA variance estimates for the random effects

[b] Correlation of BSV VC_P and $KM_PM_A = -0.667$

[c] Correlation of BSV VC_A and $CLM_A = 0.555$

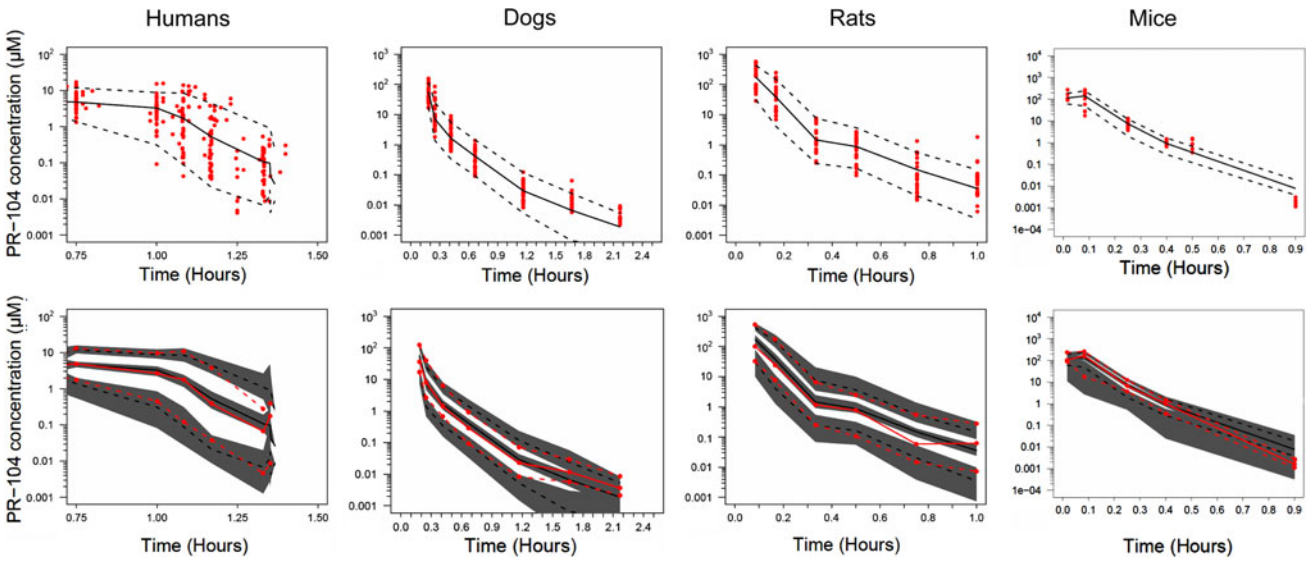

Fig. 3 Prediction-corrected visual predictive check for PR-104 in humans, dogs, rats and mice. The upper panel shows the prediction corrected observations with the predicted 5th, median and 95th percentiles. The *lower panel* shows the predicted percentiles with a 90% confidence interval (*shaded areas*) and the observed percentiles (*lines with symbols*)

the non-compartmental analysis for mice showed a 42% lower AUC of PR-104A after administration of PR-104 than PR-104A at the same molar dose (Fig. S3 and Table S4 and S5). When the mouse PK data were fitted with a compartmental model that included a separate elimination pathway for PR-104, this additional pathway accounted for 29% of PR-104 overall clearance. This is comparable to the reduction in AUC of PR-104A when derived from PR-104 noted above. However, these findings of incomplete conversion of PR-104 to PR-104A are difficult to reconcile with recent metabolite profiling and excretion studies [35], where only trace levels of unchanged PR-104 were detected in urine (humans, rats and mice) or bile (mice). Furthermore, no metabolites retaining the PR-104 phosphoryl group were observed in plasma, urine and bile [35] or in mouse normal tissues such as liver [36]. Thus, PR-104

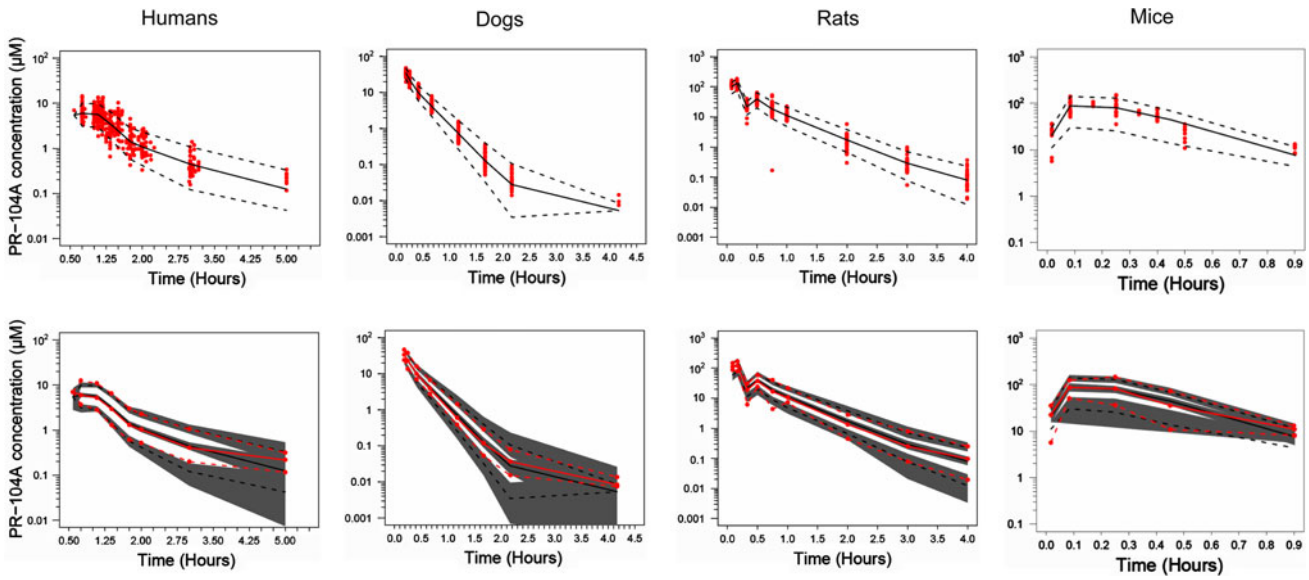

Fig. 4 Prediction-corrected visual predictive check for PR-104A in humans, dogs, rats and mice. Details are the same as Fig. 3

hydrolysis appears to be an obligatory first step in its metabolism, and its dominant elimination mechanism. Further studies are required to clarify this apparent discrepancy.

In describing the plasma PK of PR-104 itself, the compartmental model was broadly consistent with non-compartmental analysis in identifying a high PR-104 clearance in dogs. In humans, the end-of-infusion plasma concentrations of PR-104 at the MTD (~20 μM) can be used to predict a clearance of ~310 L/h/70 kg. Thus, the estimate for PR-104 clearance in humans at this concentration is faster than rats (182 L/h/70 kg) and mice (205 L/h/70 kg) but slower than dogs (1,138 L/h/70 kg). The peripheral (tissue) volume for PR-104 appeared to be lower in rodents, which may reflect species differences not accounted for by weight alone e.g. differences in body composition such as adiposity and muscle mass.

Notably, the model required a mixed-order process to describe PR-104 hydrolysis in humans but was well fitted as a first-order process in the non-human species. The presence of a saturable phosphatase pathway in humans would appear to be a robust conclusion. While this saturable hydrolysis introduces dose non-linearity for human PK, the AUC for PR-104A will still be a linear function of PR-104 dose, under the assumption that all PR-104 is converted to PR-104A. Coupled with the finding that PR-104A AUC is proportional to the logarithmic clonogenic cell killing in vitro,[1] the compartmental model implies that log tumour cell killing in vivo will be proportional to PR-104 dose. This appears to be consistent with limited data available for human tumour xenografts in mice [22].

The allometrically scaled compartmental model parameters for PR-104A showed broadly similar values for VSS_A ($VC_A + VP_A$), ranging from 105 L/70 kg in humans to 244 L/70 kg in rats. The estimate for mice (235 L/70 kg) is in reasonable agreement with the non-compartmental estimate (VSS_A = 185 L/70 kg) following dosing with PR-104A itself (Table S5). The VSS estimates for PR-104A were ~3-fold higher than for PR-104 (VSS_P ranging from 34 L/70 kg in rats to 85 L/kg in humans), which is consistent with expected restricted cellular uptake of the hydrophilic phosphate ester relative to its alcohol metabolite.

Unbound PR-104A clearances ranged from 133 to 525 L/h/70 kg (Table 3); multiplying by the unbound fractions (Table 2) gives total (bound + unbound) PR-104A clearances in the range 60–150 L/h/70 kg. Blood clearance is difficult to estimate because the blood-to-plasma ratio has not been measured. In addition, evidence that PR-104A is extensively metabolised by reduction in many normal tissues in mice [36] means it is unrealistic to relate blood clearance estimates to specific organs by comparison with blood flows.

Allometric scaling clearly identified inter-species differences in the clearance of PR-104A not accounted for by body size. Thus, the estimates of PR-104A clearance ($CLMO_A$), when adjusted to a 70-kg body weight, were 2.5-fold higher in dogs than humans, but 0.78- and 0.63-fold lower in rats and mice, respectively. Again, PR-104A itself is a minor metabolite in urine and bile [35], suggesting that the differences in clearance reflect differences in PR-104A metabolism. Concentrations of the *O*-glucuronide in dog plasma are much higher than in rodents, with humans intermediate [35], suggesting that this species difference may reflect differences in the kinetics of PR-104A glucuronidation.

As expected, BSV for $CLPM_A$ was lower in the genetically and environmentally homogeneous non-human species (31% in dogs, 28% in rats, undetectable in mice) than in humans (40%). The bioavailability of PR-104 after intraperitoneal administration to mice was estimated and indistinguishable from a model assuming bioavailability was 100%. This suggests the suitability of this dosing route for further non-human evaluation of PR-104.

An additional objective of the present study was to compare the sensitivity of each species to PR-104 toxicity, in relation to its plasma PK. The lack of cytotoxicity of PR-104 itself and the linear relationship between PR-104A AUC and probability of cell killing in culture[1] suggest that the latter is a key exposure variable. In all four species, myelosuppression is dose-limiting, but the available toxicity data (Table 1) do not provide a direct comparison across species for the same dosing schedule. Such comparisons are further complicated by the different endpoints for systemic toxicity in humans and non-human species. However, the data suggest that humans may be more sensitive to PR-104A than dogs or rats, with a lower PR-104A AUC at MTD (humans 16.9 μM h, dogs 25.1 μM h, rats 32.1 μM h), despite the use of a less dose intense (once every 3 weeks vs. weekly × 4) schedule. Mouse toxicokinetics has been evaluated less thoroughly (haematological toxicity not quantified as in the other species), but mice are able to tolerate PR-104A AUC values in the order of 100 μM h (Table 1). The PR-104A AUC values calculated from the compartmental model at MTD (humans 15.6 μM h, dogs 21.1 μM h, rats 37.8 μM h, mice 79.6 μM h) are in good agreement with non-compartmental estimates (Table 1) and include the total PK data for PR-104 available to date. We therefore conclude that mice are less sensitive to PR-104A toxicity than humans. In this respect, it is noteworthy that the human two-electron (aerobic) reductase AKR1C3 has recently been reported to activate PR-104A by reduction to its active hydroxylamine metabolite PR-104H [21]; no obvious orthologue of AKR1C3 has been identified in mice [37]. Recent evidence for AKR1C3 expression in $CD34^+$ human myeloid progenitors [38], at least at the mRNA level, suggest that local PR-104A activation in human bone marrow might contribute to this apparently higher sensitivity.

A related aim was to estimate the dose of PR-104 in non-human species which provides PR-104A exposure equivalent to that achievable in humans. The use of doses in mice giving plasma concentrations higher than humans is a recognised problem in cancer pharmacology and a likely contributor to over-prediction of activity against xenografts relative to that in humans [39]. As noted above, the compartmental model indicated that the PR-104A AUC will be a linear function of dose in all species. Thus, the PR-104 dose in non-human species providing PR-104A AUC equivalent to that in humans can be calculated using the ratio of clearances of PR-104A (CL_A) in non-human species to that in humans (Eq. 3):

$$\text{Human-equivalent dose} = \text{human dose} \times \frac{CL_A, \text{non-human}}{CL_A, \text{human}} \quad (3)$$

In Eq. 3, CL_A is the PR-104A clearance for the whole animal (L/h) and can be calculated from the species-specific allometric clearances per 70 kg ($CLMO_A$ in Table 3) by Eq. 4:

$$CL_A = CLMO_A \times (BW/70)^{0.75} \quad (4)$$

where the body weight (BW) is in kg. The allometric model developed here provides estimates of *the ratio of CL_A clearances* (non-human/human) of 0.578 for dogs, 0.0096 for rats and 0.00164 for mice following single i.v. doses (or i.p. doses in mice). Thus, for the single-agent human MTD of 1,100 mg/m^2 (1,903 mg for a 70-kg individual), an iso-AUC dose in mice is estimated to be 3.12 mg for a 25-g mouse, or 125 mg/kg, which is approximately 25% of the MTD in mice for a single i.v. dose (Table 1). Future studies with PR-104 in non-human species must account for this substantial species difference in PR-104A PK and examine a dose range consistent with expected human exposure.

Acknowledgments We thank Proacta Inc. for provision of PR-104 and access to pharmacokinetic and toxicity data for rats, dogs and humans, and MicroConstants Inc. for assay of PR-104 and PR-104A in plasma from these species. The study was supported by grant 08/103 from the Health Research Council of New Zealand and a Fellowship to KP from the Auckland Medical Research Foundation.

William R. Wilson is a founding scientist, stockholder and consultant to Proacta, Inc.

References

1. Carmeliet P (2005) Angiogenesis in life, disease and medicine. Nature 438:932–936
2. Liao D, Johnson RS (2007) Hypoxia: a key regulator of angiogenesis in cancer. Cancer Metastasis Rev 26:281–290
3. Kioi M, Vogel H, Schultz G, Hoffman RM, Harsh GR, Brown JM (2010) Inhibition of vasculogenesis, but not angiogenesis, prevents the recurrence of glioblastoma after irradiation in mice. J Clin Invest 120:694–705
4. Erler JT, Giaccia AJ (2006) Lysyl oxidase mediates hypoxic control of metastasis. Cancer Res 66:10238–10241
5. O'Donnell JL, Joyce MR, Shannon AM, Harmey J, Geraghty J, Bouchier-Hayes D (2006) Oncological implications of hypoxia inducible factor-1alpha (HIF-1alpha) expression. Cancer Treat Rev 32:407–416
6. Bristow RG, Hill RP (2008) Hypoxia, DNA repair and genetic instability. Nat Rev Cancer 8:180–192
7. Gatenby RA, Gillies RJ (2007) Glycolysis in cancer: a potential target for therapy. Int J Biochem Cell Bio 39:1358–1366

8. Koong AC, Chauhan V, Romero-Ramirez L (2006) Targeting XBP-1 as a novel anti-cancer strategy. Cancer Biol Ther 5:756–759
9. Graeber TG, Osmanian C, Jacks T, Housman DE, Koch CJ, Lowe SW, Giaccia AJ (1996) Hypoxia-mediated selection of cells with diminished apoptotic potential in solid tumours. Nature 379:88–91
10. Brown JM, Wilson WR (2004) Exploiting tumor hypoxia in cancer treatment. Nat Rev Cancer 4:437–447
11. Tatum JL, Kelloff GJ, Gillies RJ, Arbeit JM, Brown JM, Chao KS, Chapman JD, Eckelman WC, Fyles AW, Giaccia AJ, Hill RP, Koch CJ, Krishna MC, Krohn KA, Lewis JS, Mason RP, Melillo G, Padhani AR, Powis G, Rajendran JG, Reba R, Robinson SP, Semenza GL, Swartz HM, Vaupel P, Yang D, Croft B, Hoffman J, Liu G, Stone H, Sullivan D (2006) Hypoxia: importance in tumor biology, noninvasive measurement by imaging, and value of its measurement in the management of cancer therapy. Int J Radiat Biol 82:699–757
12. Stratford IJ, Workman P (1998) Bioreductive drugs into the next millennium. Anticancer Drug Des 13:519–528
13. Denny WA (2001) Prodrug strategies in cancer therapy. Eur J Med Chem 36:577–595
14. Wardman P (2001) Electron transfer and oxidative stress as key factors in the design of drugs selectively active in hypoxia. Curr Med Chem 8:739–761
15. McKeown SR, Cowen RL, Williams KJ (2007) Bioreductive drugs: from concept to clinic. Clin Oncol 19:427–442
16. Chen Y, Hu L (2009) Design of anticancer prodrugs for reductive activation. Med Res Rev 29:29–64
17. Jameson MB, Rischin D, Pegram M, Gutheil J, Patterson AV, Denny WA, Wilson WR (2010) A phase I pharmacokinetic trial of PR-104, a nitrogen mustard prodrug activated by both hypoxia and aldo-keto reductase 1C3, in patients with solid tumors. Cancer Chemother Pharmacol 65:791–801
18. Patterson AV, Ferry DM, Edmunds SJ, Gu Y, Singleton RS, Patel K, Pullen SM, Syddall SP, Atwell GJ, Yang S, Denny WA, Wilson WR (2007) Mechanism of action and preclinical antitumor activity of the novel hypoxia-activated DNA crosslinking agent PR-104. Clin Cancer Res 13:3922–3932
19. Singleton RS, Guise CP, Ferry DM, Pullen SM, Dorie MJ, Brown JM, Patterson AV, Wilson WR (2009) DNA crosslinks in human tumor cells exposed to the prodrug PR-104A: relationships to hypoxia, bioreductive metabolism and cytotoxicity. Cancer Res 69:3884–3891
20. Guise CP, Wang A, Thiel A, Bridewell D, Wilson WR, Patterson AV (2007) Identification of human reductases that activate the dinitrobenzamide mustard prodrug PR-104A: a role for NADPH:cytochrome P450 oxidoreductase under hypoxia. Biochem Pharmacol 74:810–820
21. Guise CP, Abbattista M, Singleton RS, Holford SD, Connolly J, Dachs GU, Fox SB, Pollock R, Harvey J, Guilford P, Doñate F, Wilson WR, Patterson AV (2010) The bioreductive prodrug PR-104A is activated under aerobic conditions by human aldo-keto reductase 1C3. Cancer Res 70:1573–1584
22. Hicks KO, Myint H, Patterson AV, Pruijn FB, Siim BG, Patel K, Wilson WR (2007) Oxygen dependence and extravascular transport of hypoxia-activated prodrugs: comparison of the dinitrobenzamide mustard PR-104A and tirapazamine. Int J Radiat Oncol Biol Phys 69:560–571
23. Wilson WR, Hicks KO, Pullen SM, Ferry DM, Helsby NA, Patterson AV (2007) Bystander effects of bioreductive drugs: potential for exploiting pathological tumor hypoxia with dinitrobenzamide mustards. Radiat Res 167:625–636
24. Liu SC, Ahn GO, Kioi M, Dorie MJ, Patterson AV, Brown JM (2008) Optimised Clostridium-directed enzyme prodrug therapy improves the antitumor activity of the novel DNA crosslinking agent PR-104. Cancer Res 68:7995–8003
25. Patel K, Lewiston D, Gu Y, Hicks KO, Wilson WR (2007) Analysis of the hypoxia-activated dinitrobenzamide mustard phosphate prodrug PR-104 and its alcohol metabolite PR-104A in plasma and tissues by liquid chromatography-mass spectrometry. J Chromatogr B Analyt Technol Biomed Life Sci 856:302–311
26. Gu Y, Wilson WR (2009) Rapid and sensitive ultra-high-pressure liquid chromatography-tandem mass spectrometry analysis of the novel anticancer agent PR-104 and its major metabolites in human plasma: application to a pharmacokinetic study. J Chromatogr B Analyt Technol Biomed Life Sci 877:3181–3186
27. Jameson MB, McKeage MJ, Ramanathan RK, Rajendran J, Gu Y, Wilson WR, Melink TJ, Tchekmedyian NS (2010) Final results of a phase Ib trial of PR-104, a pre-prodrug of the bioreductive prodrug PR-104A, in combination with gemcitabine or docetaxel in patients with advanced solid tumors. ASCO Meeting Abstracts (Abstract 2554)
28. Anderson BJ, Holford NHG (2008) Mechanism-based concepts of size and maturity in pharmacokinetics. Ann Rev Pharmacol Toxicol 48:303–332
29. Denny WA, Atwell GJ, Yang S, Wilson WR, Patterson AV, Helsby NA (2005) Novel nitrophenyl mustard and nitrophenylaziridine alcohols and their corresponding phosphates and their use as targeted cytotoxic agents. PCT WO2005042471A1
30. Holford NHG (1996) A size standard for pharmacokinetics. Clin Pharmacokinet 30:329–332
31. West GB, Brown JH, Enquist BJ (1997) A general model for the origin of allometric scaling laws in biology. Science 279:122–126
32. West GB, Brown JH, Enquist BJ (1999) The fourth dimension of life: fractal geometry and allometric scaling of organisms. Science 284:1677–1679
33. Anderson BJ, Woollard GA, Holford NHG (2000) A model for size and age changes in the pharmacokinetics of paracetamol in neonates, infants and children. Br J Clin Pharmacol 502:125–134
34. Kolokotrones T, Savage V, Deeds EJ, Fontana W (2010) Curvature in metabolic scaling. Nature 464:753–756
35. Gu Y, Atwell GJ, Wilson WR (2010) Metabolism and excretion of the novel bioreductive prodrug PR-104 in mice, rats, dogs and humans. Drug Metab Dispos 38:498–508
36. Gu Y, Guise CP, Patel K, Abbattista MR, Lie J, Sun X, Atwell GJ, Boyd M, Patterson AV, Wilson WR (2010) Reductive metabolism of the dinitrobenzamide mustard anticancer prodrug PR-104 in mice. Cancer Chemother Pharmacol. doi:10.1007/s00280-010-1354-5
37. Velica P, Davies NJ, Rocha PP, Schrewe H, Ride JP, Bunce CM (2009) Lack of functional and expression homology between human and mouse aldo-keto reductase 1C enzymes: implications for modelling human cancers. Mol Cancer 8:121–132
38. Birtwistle J, Hayden RE, Khanim FL, Green RM, Pearce C, Davies NJ, Wake N, Schrewe H, Ride JP, Chipman JK, Bunce CM (2009) The aldo-keto reductase AKR1C3 contributes to 7, 12-dimethylbenz(a)anthracene-3, 4-dihydrodiol mediated oxidative DNA damage in myeloid cells: implications for leukemogenesis. Mutat Res 662:67–74
39. Peterson JK, Houghton PJ (2004) Integrating pharmacology and in vivo cancer models in preclinical and clinical drug development. Eur J Cancer 40:837–844